Tanycytic VEGF-A Boosts Blood-Hypothalamus Barrier Plasticity and Access of Metabolic Signals to the Arcuate Nucleus in Response to Fasting

Fanny Langlet, Barry E. Levin, Serge Luquet, Massimiliano Mazzone,
Andrea Messina, Ambrose A. Dunn-Meynell, Eglantine Balland, Amelie
Lacombe, Daniele Mazur, Peter Carmeliet, et al.

Glucose and tanycyte-derived VEGF-A promote blood-hypothalamus barrier plasticity and access of blood-borne molecules to the arcuate nucleus in response to fasting

Fanny Langlet,[1,2,3] **Barry E. Levin,**[4,5,‡] **Serge Luquet,**[6,‡] **Massimiliano Mazzone,**[7,‡] **Andrea Messina,**[1,2,3,‡] **Ambrose A. Dunn-Meynell,**[4,5] **Eglantine Balland,**[1,2,3] **Amelie Lacombe,**[6] **Daniele Mazur,**[1,2,3] **Peter Carmeliet**[7]**, Sebastien G. Bouret,**[1,2,3,8] **Vincent Prevot,**[1,2,3*] **Bénédicte Dehouck**[1,2,3,9]

[1] Inserm, Jean-Pierre Aubert Research Centre, U837, Development and plasticity of the postnatal brain, F-59000 Lille, France
[2] UDSL, School of Medicine, Lille, F-59000, France
[3] Univ Lille Nord de France, Institut de Médecine Prédictive et de Recherche Thérapeutique, F-59000 Lille, France
[4] Neurology Service, Veterans Affairs Medical Center, East Orange, NJ 07018-1095, USA
[5] Department of Neurology and Neurosciences, New Jersey Medical School, University of Medicine and Dentistry of New Jersey, Newark, NJ 07103, USA
[6] Univ Paris Diderot, Sorbonne Paris Cité, BFA, EAC 4413 CNRS, F-75205 Paris, France
[7] VIB Vesalius Research Center, University of Leuven, B-3000 Leuven, Belgium
[8] Neuroscience Program, The Saban Research Institute, Childrens Hospital Los Angeles, University of Southern California, Los Angeles, CA 90027, USA
[9] Université d'Artois, F-62800 Liévin, France

[‡] These authors contributed equally to this work

Running Title: Hypothalamic barriers in CNS control of feeding

Number of text pages: 24
Number of figures: 4
Number of tables: 0

* Corresponding author: Vincent Prevot, Ph.D., Inserm 837, Bâtiment Biserte,
Place de Verdun, 59045 Lille Cedex, France
Tel : +33 320-62-20-64
Fax : +33 320-53-85-62
E-mail : vincent.prevot@inserm.fr

Summary

The delivery of blood-borne molecules conveying metabolic information to neural networks that regulate energy homeostasis is restricted by brain barriers. The fenestrated endothelium of median eminence microvessels and tight junctions between tanycytes together compose one of these. Here, we show that the decrease in blood glucose levels during fasting alters the structural organization of this blood-hypothalamus barrier, resulting in the improved access of metabolic substrates to the arcuate nucleus. These changes are mimicked by 2-deoxyglucose-induced glucoprivation and reversed by raising blood glucose levels after fasting. Furthermore, we show that VEGF-A expression in tanycytes modulates these barrier properties. The neutralization of VEGF signaling blocks fasting-induced barrier remodeling and significantly impairs the physiological response to refeeding. These results implicate glucose in the control of blood-hypothalamus exchanges through a VEGF-dependent mechanism, and demonstrate a hitherto unappreciated role for tanycytes and the permeable microvessels associated with them in the adaptive metabolic response to fasting.

Introduction

Appetite, energy balance and metabolism are all controlled by select neurons of the hypothalamic arcuate nucleus (ARH) (see for reviews (Elmquist et al., 2005; Gao and Horvath, 2007; Levin et al., 2011; Sawchenko, 1998)). These interoceptive sensory neurons participate in neural networks that sense circulating factors such as glucose and adiposity hormones that signal changes in metabolic state (Cowley et al., 2001; Cowley et al., 2003; Dunn-Meynell et al., 2002; Elias et al., 1999; Hill et al., 2010; Liu et al., 2012). However, the physiological mechanisms that control the access of these factors to ARH circuits and their regulation in response to changes in feeding status remain largely unexplored.

Molecular traffic between the periphery and the central nervous system (CNS), including the hypothalamus, is restricted by regulated interfaces, such as the blood-brain barrier (BBB), composed of tight junctions between endothelial cells lining brain microvessels (Neuwelt et al., 2011). The blood-cerebrospinal-fluid (CSF) barrier, a lesser known interface, is composed of tanycytes, specialized hypothalamic glia that line the floor of the 3rd ventricle, and microvessels of the median eminence (ME), a circumventricular organ adjacent to the ARH (Mullier et al., 2010). While the endothelial cells of the ME are unique in being fenestrated, and thus highly permeable to blood-borne molecules, tight junction complexes between adjacent tanycytes act as a physical barrier preventing their diffusion to the rest of the brain via the CSF. Transcellular transport across the blood-brain and blood-CSF barriers is usually mediated by saturable carriers (Banks, 2006; Hawkins and Davis, 2005). However, whether specific hypothalamic areas that regulate energy balance, such as the ARH, directly access peripheral homeostatic signals through the fenestrated microvessel plexus in the adjacent ME is a matter of debate (Ciofi et al., 2009; Flier, 2004; Mullier et al., 2010).

Here we show that food deprivation, by inducing both tight junction complex reorganization in tanycytes and the increased fenestration and permeability of ME microvessel loops that reach the ventromedial ARH (vmARH) (Ambach and Palkovits, 1979), leads to such direct access. Refeeding, glucose infusion, the selective inhibition of vascular

endothelial growth factor (VEGF)-A expression in tanycytes and the manipulation of VEGF signaling all reverse these structural changes and the resulting ability of molecules to enter the ARH.

Results

Fasting-induced plasticity of the blood-hypothalamus barrier (BHB)

To investigate the role of BHB plasticity in the adaptive response to fasting, we compared the hypothalami of mice deprived of food for 24h and those fed *ad libitum* using immunofluorescence for two constitutive tight junction proteins, zonula occludens-1 (ZO-1) and occludin, expressed in BBB endothelial cells and tanycytes, and claudin-1, expressed in tanycytes at the blood-CSF barrier (Mullier et al., 2010). In parallel, antibodies to MECA-32 were used to selectively label the fenestral diaphragms of ME endothelial cells (Ciofi et al., 2009; Mullier et al., 2010).

Fasting increased the organization of tanycytic tight junction complexes in both the ME and ARH (Fig. 1A,B; Fig. S1A), but not in standard non-ARH hypothalamic vessels composing the BBB (Fig. S1B). Fasting intensified the honeycomb-like pattern of ZO-1 and occludin around the apical pole of tanycytes overlying the ME (Fig. 1A, insets 2,5; Fig. S1A, insets 3,6), and switched ZO-1 and occludin distribution from a diffuse apical pattern to a honeycomb pattern in tanycytes lining the third ventricle (3V) next to the ARH (Fig. 1A, insets 1,4; Fig. S1A, insets 2,5). Claudin-1 expression in ARH tanycytes also became organized in food-deprived mice (Fig. 1C,D). This reorganization was associated with increased protein levels of ZO-1, but not of occludin or claudin-1, in fasting animals (Fig. S1D). Finally, food-deprived mice refed for an additional 24h displayed a reappearance of the hypothalamic barrier phenotype of fed mice (Fig. 1B-D).

In fasting mice, ME microvessel loops, some of which extend up to the ARH, also demonstrated a marked increase in fenestration associated with changes in MECA-32 distribution (Fig. 1A, insets 1,4; Fig. 1B) and the appearance of fenestrated diaphragms at the ultrastructural level (Fig. 1E, inset 2; Fig. S1C). Western blotting revealed that this increased fenestration was accompanied by a significant increase in MECA-32 protein levels ($p < 0.05$; Fig. 1F). Together, the fasting-induced structural reorganization of the tight junction complexes of tanycytes lining the ventricular wall adjoining the ARH potentially limits

paracellular diffusion between the tissue and the CSF, while ME microvessels simultaneously become more leaky. These reversible morphological alterations at the BHB suggest that nutritional state modulates the access of metabolic signals from the periphery to ARH neurons critical for energy homeostasis.

Glucose deprivation mediates fasting-induced plasticity at the BHB

What nutritional factors underlie these profound morphological changes in fasting mice? Blood glucose acts as a metabolic signal that can alter the activity of hypothalamic neurons (Levin et al., 2011; Thorens and Larsen, 2004) and evokes robust signaling in tanycytes, which act as glucosensors (Frayling et al., 2011), suggesting that reduced glucose levels could underlie the morphological changes seen during fasting. As expected, blood glucose levels were significantly lower after 24h of food deprivation (Fig. 2A, p<0.001). Levels were normalized and fasting-induced BHB reorganization prevented (Fig. 2B) by intravenous (i.v.) glucose (30%, 1-3 µl/min; n = 6) but not saline infusion (n = 4). On the other hand, central neuroglucopenia induced by the intraperitoneal (i.p.) or intracerebroventricular (i.c.v.) injection of 2-deoxy-D-glucose (2-DG, 300 mg/kg i.p. or 1 mg/mouse i.c.v.; n = 4 each, Fig. 2B; Fig. S2A), a glucose analog that inhibits glucose metabolism but can act on tanycytes (Frayling et al., 2011), caused the reorganization of tanycytic tight junction complexes and associated microvessel loops to resemble those in fasting mice. The central detection of glucose deprivation thus appears to play a key role in BHB reorganization after fasting.

VEGF promotes changes in ME microvessel loops and tanycytic tight junction complexes during fasting

Quantitative RT-PCR analyses showed that fasting induced a constellation of hypothalamic transcripts involved in controlling the structural plasticity of the brain (Fig. 2C). However, only VEGF-A expression was upregulated in both fasting and 2-DG-treated animals (Fig. 2C). VEGF protein levels increased in the hypothalamus of 24h-fasting mice when compared to fed mice (p<0.05; Fig. 2D), and 2DG-treatment for 12h directly triggered VEGF secretion

from ME-ARH explants *in vitro* (p<0.05; Fig. 2E). We therefore treated mice for 24h with Axitinib (25 mg/kg/12h, i.p. or 70 μg/mouse, i.c.v.), a tyrosine kinase inhibitor that selectively inhibits VEGF receptors (VEGFR) 1, 2 and 3 (Mancuso et al., 2006). Axitinib reversed both fasting- and 2DG-evoked changes in tight junction complex organization in tanycytes and the associated microvessel loops in the ME/ARH region (Fig. 2B,F; Fig. S2A,B). Conversely, VEGF infusion (60 μg/kg/12h, i.p. or 100 ng/mouse, i.c.v.) for 24h mimicked the effects of fasting on BHB plasticity in fed mice (Fig. 2F,G; Fig. S2B) without affecting tight junction organization in BBB capillaries (Fig. S1B).

Next, we examined the contribution of VEGFR1, 2 and 3, which are all expressed in the mediobasal hypothalamus (MBH; Fig. S2C), to fasting-induced BHB plasticity, by administering selective neutralizing monoclonal antibodies to each receptor (40 mg/kg, i.p.) (Pytowski et al., 2005; Wang et al., 2004). While antibodies to VEGFR1 and 3 bound to both hypothalamic BBB microvessels and the ME microvessel plexus, antibodies to VEGFR2 bound only to the latter (Fig. S2D). Importantly, the blockade of VEGFR2 and, to a lesser extent, VEGFR1, inhibited the BHB rearrangement observed after fasting (Fig. S2E,F), while antibodies to VEGFR3 had no effect on this plasticity (Fig. S2F). Together, these data suggest that increased hypothalamic VEGF levels during food deprivation target VEGFR1 and 2 in ME endothelial cells to promote microvessel permeability and tight junction complex reorganization in the ME and ARH.

Fasting-induced BHB plasticity requires tanycytic VEGF-A expression

VEGF-A mRNA expression in the hypothalamic tuberal region is restricted to tanycytes (Allen Brain atlas, http://mouse.brain-map.org/experiment/show/74988747, Fig. S3A), suggesting that these cells play a role in the control of VEGF-mediated BHB plasticity. Cell sorting experiments using *tdTomato*[loxP/+] reporter mice in which the tat-cre fusion protein, whose cellular uptake is enhanced compared to cre recombinase (Peitz et al., 2002), was stereotaxically infused into the 3rd ventricle, where it selectively targeted tanycytes (Fig. S2G), to study fasting-dependent changes in tanycytic gene expression *in vivo* (Fig. 2H).

Sorted Tomato-positive cells abundantly expressed the tanycytic marker DARPP-32 (Hokfelt et al., 1988), which was barely detectable in Tomato-negative cells (Fig. S2I). Purified tanycytes also expressed GLUT1, GLUT2 and glucokinase transcripts, as suggested by others (Rodriguez et al., 2005), and low levels of VEGFR1 and 2, although VEGFR3 was undetectable (Fig. S2I). Intriguingly, fasting upregulated VEGF-A but not VEGF-B or VEGF-C mRNA expression in tanycytes (Fig. 2H; Fig. S2J), with a concomitant increase in the transcript for hypoxia-inducible factor 1 alpha (HIF-1α) (Fig. S2K), recently shown to be involved in hypothalamic glucosensing (Zhang et al., 2011) and known to promote VEGF expression (Carmeliet et al., 1998). Finally, *Vegfa* deletion in tanycytes by tat-cre infusion into the third ventricle of *Vegfa*$^{loxP/loxP}$ mice (Fig. S3A) abolished fasting-induced BHB reorganization (n = 4; Fig. 2F) but did not affect BHB properties in animals fed *ad libitum* (n = 4; not shown). Together these data demonstrate that tanycytic VEGF-A expression plays a key role in regulating fasting-induced BHB plasticity.

BHB plasticity modulates the access of blood-borne metabolic factors to the ARH

To establish whether the morphological changes described in the MBH above were associated with altered permeability and access of blood-borne molecules to the ARH, the extravasation of intravenously-injected Evans Blue dye from brain microvessels into the hypothalamus was compared between 24h-fasting and fed mice. In fed mice, Evans Blue diffusion was restricted to the vascular bed of hypothalamic BBB microvessels and the ME (Fig. 3A, top panels), and did not spread to neighboring structures such as the ARH. In striking contrast, in 24h-fasting mice, the dye was observed in the ventromedial ARH (vmARH), where plastic BHB changes were observed in previous experiments (Fig. 3A,B). As with the morphological changes, refeeding reversed dye diffusion into the vmARH (Fig. 3B). Importantly, fasting did not promote dye extravasation from the intrinsic hypothalamic microvessels that compose the BBB (Fig. S3B). The inhibition of BHB reorganization in food-deprived mice by Axitinib, VEGFR2-neutralizing antibodies, *Vegfa* gene targeting or glucose infusion prevented dye diffusion into the ARH, whereas the induction of barrier plasticity with

VEGF in fed mice clearly elicited such diffusion (Fig. 3B). These findings strongly suggest that the anatomical changes at the BHB in fasting animals facilitate the access of blood-borne signals to the vmARH due to its increased permeability.

To directly test whether fasting-induced structural rearrangements at the BHB do indeed increase the access of critical metabolic substrates to the ARH, we simultaneously assessed glucose levels in the ARH and the adjacent ventromedial nucleus of the hypothalamus (VMH) by microdialysis in fed or 24h-fasting rats (Fig. 3C). First, rats exhibited similar fasting-induced morphological and functional changes to the BHB as did mice (Fig. S3C-E). While ARH glucose levels in fed rats were comparable to those in the VMH (Fig. 3C), in 24h-fasting rats, ARH glucose levels were 300% higher than VMH levels (Fig. 3C). In keeping with the restricted occurrence of microvessels whose permeability changes in response to feeding status in the vmARH, and unlike what would have been expected if the BBB were completely permeable throughout the ARH, ARH glucose levels during fasting ($\approx$ 2mM) never reached blood levels ($\approx$ 5mM). However, these data do suggest that fasting-induced structural changes at the BHB create a privileged route for the access of circulating glucose to glucosensing ARH neurons, bypassing both the BBB and the blood-CSF barrier (Fig. 3F).

We further explored this hypothesis by examining the ability of exogenous leptin, a 16-kDa peptide hormone, to access ARH neurons by quantifying the leptin-stimulated phosphorylation of STAT3 in fasting and fed mice. Leptin (3 mg/kg, i.p.) induced a 30% increase in immunoreactivity for phosphorylated STAT3 (pSTAT3) in food-deprived mice when compared to fed mice (Fig. 3D). This increase was restricted to the vmARH (Fig. S3F). Axitinib (which inhibits BHB rearrangement; Fig. 2F) prevented the leptin-induced increase in pSTAT3 in fasting animals (Fig. 3D,E). Conversely, the treatment of fed mice (in which endogenous leptin levels are significantly higher than in fasting mice; Fig. S3G), with VEGF, which promotes BHB reorganization (Fig. 2F,G), markedly increased STAT3 activation in the ARH (Fig. 3D,E). This effect was blunted by the i.p. injection of a mutated recombinant leptin antagonist (LAN; 3 mg/kg) that is devoid of biological activity but effectively binds to the leptin

receptor (Niv-Spector et al., 2005) 45 min before death (Fig. 3D,E), suggesting that leptin access to the ARH is facilitated by VEGF treatment in fed mice. Together, these data suggest an important role for BHB plasticity in modulating the access of metabolic factors to the ARH.

BHB plasticity modulates feeding

To evaluate the functional consequences of BHB plasticity to feeding behavior, we measured refeeding after fasting in control and Axitinib-treated mice. Compared to vehicle-infused mice refed after a 24h fast, food intake was significantly lower in Axitinib-treated refed mice (Fig. 4A). This difference, which occurred primarily during the first 30 min of refeeding (Fig. 4A), was associated with decreased body weight gain 24h and 48h after Axitinib administration (Fig. 4B). Importantly, Axitinib alone did not inhibit food intake in animals fed *ad libitum* (Fig. 4A), suggesting that reduced feeding in fasting mice was not due to food aversion. Conversely, food intake significantly increased in the afternoon and at lights-off (when endogenous anorectic hormones are thought to stimulate food intake) in fed mice 24h after the initiation of VEGF treatment, when compared to vehicle-treated mice (Fig. 4C). Subsequently, we found that the anorectic and weight-loss-inducing effects of exogenous leptin were greater in fed mice treated with VEGF than in vehicle-treated controls (Fig. 4D). Together, these findings suggest that VEGF-mediated structural changes at the BHB, by modulating the access of blood-borne metabolic substrates to the ARH, play an important role in the adaptive response to fasting.

Discussion

Energy homeostasis requires increased food intake when energy stores are depleted, and a means of signaling this depletion to central neurons that control feeding behavior (Cowley et al., 2001; Cowley et al., 2003; Dunn-Meynell et al., 2002; Elias et al., 1999; Liu et al., 2012), such as ARH neurons (Hill et al., 2010). Here, we provide evidence that the BHB (Mullier et al., 2010) undergoes dynamic and reversible structural changes that modulate its permeability in response to glucose and tanycytic VEGF levels, thereby acting as a checkpoint in the access of peripheral metabolic signals to ARH neurons.

Our data show that fasting-evoked dips in blood glucose levels trigger VEGF-A expression in tanycytes and VEGF accumulation in the hypothalamic ME, which acts via VEGFR to promote endothelial cell fenestration. Tanycytes contacting these newly permeable microvessel loops then reorganize their tight junction complexes to seal the paracellular space between the parenchyma and the CSF. In consequence, some target neurons in the vmARH are no longer insulated by the blood-brain and blood-CSF barriers but become directly exposed to peripheral metabolic signals (Fig. 3F), a situation reversed upon refeeding. This increased accessibility is confirmed both by the leakage of intravenously injected dye into the vmARH and by higher physiological glucose levels in the ARH than in the adjacent VMH in the fasting state. Fasting-induced reorganization is blocked by the VEGFR inhibitor Axitinib, which, consistent with the importance of these changes in the adaptive response to fasting, reduces food intake and weight gain when food-deprived mice are refed. Even though Axitinib alone did not affect food intake in control animals fed *ad libitum*, chronic Axitinib treatment, which causes a marked reduction in endothelial cell (Kamba et al., 2006), is known to affect glucose homeostasis (Kamba et al., 2006) and to lead to decreased appetite and weight loss in patients (Fruehauf et al., 2011; Rini et al., 2009).

Conversely, triggering BHB permeability in mice fed *ad libitum* with exogenous VEGF, which signals food deprivation, significantly increases their food intake and sensitivity to the

anorectic effects of leptin. We used leptin as a surrogate for other large metabolic peptides such as ghrelin because we could assess its access to the vmARH by monitoring the activation of STAT3. In fact, leptin levels are decreased during fasting, leading to a marked anabolic state within the hypothalamus, with increased neuropeptide Y and agouti-related peptide (AgRP) and decreased proopiomelanocortin levels. This combination acts as a potent stimulus for the animal to seek and ingest food. Contrarily, ghrelin levels increase during fasting, and the increased permeability of ARH microvessels to this peptide could facilitate its selective activation of anabolic AgRP neurons (Elmquist et al., 2005; Gao and Horvath, 2007; Levin et al., 2011; Sawchenko, 1998).

Falling blood glucose levels and decreased glucose metabolism appear to be critical signals for the initiation of the BHB response to starvation. Glucose replacement prevents this rearrangement while 2-DG-induced central glucopenia reproduces it. The molecular pathways that underlie the subsequent accumulation of VEGF in the ME are unknown. However, our results showing that VEGF-A inactivation in these cells blunts fasting-induced BHB plasticity strongly suggest that they are intrinsic to tanycytes, which directly and rapidly respond to changes in glucose levels (Frayling et al., 2011). This response could involve HIF-1α, which is upregulated in tanycytes by fasting (Fig. S2J), and is known to be activated by glucoprivation and to promote VEGF expression (Carmeliet et al., 1998; Zhang et al., 2011).

VEGF has long been associated with increased vascular permeability (Esser et al., 1998; Ioannidou et al., 2006) and is required for ependymal cell function and the maintenance of key brain-periphery interfaces such as the choroid plexus (Maharaj et al., 2008). VEGF might also contribute to increased BBB permeability in diseased (Argaw et al., 2009) but not healthy brains (Hawkins et al., 2010) (Fig. S1B; Fig. S3A). Our data suggest that VEGF and its signaling receptor, VEGFR2, are key determinants of fasting-induced structural rearrangements at the BHB. Although VEGF involvement in endothelial cell fenestration and the expression of diaphragm proteins (named PV-1 in rats and MECA-32 in mice) is clearly documented (Esser et al., 1998; Kamba et al., 2006), the mechanisms underlying tight-

junction-complex remodeling in tanycytes, which express low levels of VEGFR2, are unknown. These could also involve VEGF signaling, which induces posttranslational modifications in tight junction proteins under some pathological conditions (Murakami et al., 2009), or other as-yet undiscovered signals released by endothelial cells upon fenestration.

Tight junction proteins such as occludin, whose organization is modified in tanycytes under fasting conditions, could also be involved in brain metabolic sensing and body-weight regulation. Occludin-null mice are leaner than their wild-type littermates (Saitou et al., 2000), and the i.c.v. infusion of antisense oligodeoxynucleotides to occludin restores leptin sensitivity in an animal model of diet-induced leptin resistance and hyperglycemia (Oh et al., 2005) in which fasting appears not to promote changes in BHB permeability (unpublished observations). This, together with recent findings showing that a high-fat diet triggers neurogenic activity in ME tanycytes (Lee et al., 2012), shows that these cells play a dynamic role in metabolic sensing and hold therapeutic potential in metabolic disorders.

Overall our data unveil a new physiological concept in the maintenance of energy homeostasis, in which blood glucose levels, by regulating tanycytic VEGF-A expression, modulate the organization of their tight junctions as well as the permeability of ME capillary loops in the vmARH, and thereby control the access of circulating homeostatic signals to brain circuits that regulate metabolism.

Experimental procedures

Animals

Male C57Bl/6 mice, 3-4 months old (Charles River, France) and male Sprague Dawley rats (Charles River, USA) were given *ad libitum* access to water and standard laboratory chow. *tdTomato*$^{loxP/+}$ reporter mice were purchased from the Jackson laboratories (Maine, USA) and *Vegfa*$^{loxP/loxP}$ mice (Gerber et al., 1999) were a gift from N. Ferrara (Novartis, USA). Animal studies were approved by the Institutional Animal Care and Use Committee of Lille and the East Orange Veterans Affairs Medical Center.

Treatment protocols

Glucose infusion and 2-deoxy-D-glucose (2-DG) injection. Mice fed *ad libitum* and fasting mice were anesthetized with isoflurane and the jugular vein catheterized. After a 7-day recovery period, fed mice were infused with saline solution (0.9%) for 24h while fasting mice were infused with glucose (30% in saline) or saline. Moreover, mice fed *ad libitum* were given an i.p. or i.c.v. injection of 2-DG (RDS, France) in saline or an equal volume of saline alone, following procedures described previously (Mullier et al., 2010).

Anti-VEGF and VEGF treatments. Mice were subjected to an i.p. or i.c.v. infusion of Axitinib (in DMSO, LC Laboratories, France) or an equal volume of DMSO during the 24h fasting period. Finally, mice fed *ad libitum* were given an i.p. or i.c.v. infusion of recombinant mouse VEGF 164 (RDS, France) in PBS for 24h.

Tat-cre delivery. A tat-cre fusion protein produced as detailed previously (Peitz et al., 2002) was stereotaxically infused into the third ventricle (1.5 µl over 5 min at 2.1 mg/ml; AP: -1.7 mm, ML: 0 mm DV: - 5.6 mm) of isoflurane-anesthetized floxed mice 24h before experiments.

Fluorescence-activated cell-sorting and real-time PCR analyses

Tomato-positive cells were sorted and collected from ME explants microdissected from fasting and fed mice and processed for quantitative RT-PCR, as described in the Supplemental Experimental Procedures.

Physiological measurements

Food intake. Mice were housed 3 per cage with preweighed amounts of food dispensed through the wire cage tops, and food intake was measured every 30 min for the first 3 hours and every hour for 24 hours. The average and cumulative food intake of 3 mice was used for statistical comparisons (n = 4 cages per group).

In vivo leptin sensitivity test. Mice were housed in individual cages two days before the beginning of the experiment. Mice fed *ad libitum* and fed mice infused with VEGF were injected i.p. at 18:00 with vehicle (5 mM sodium citrate buffer, pH 4.0) or leptin (3 mg/kg, PeproTech, France). Body weight and food consumption were measured at 08:00 the next day.

Permeability assays, immunohistochemistry and image analysis

Mice were given i.v. injections of sterile 1% Evans Blue dye (Sigma, France) in 0.9% saline (50 µl) into the tail vein and killed by decapitation 20 min later. Brains were processed for immunofluorescence as described previously (Mullier et al., 2010). The primary antibodies used were: polyclonal rabbit anti-zonula occludens-1 (ZO-1, 1:500, Zymed, USA), rabbit anti-claudin-1 (1:200, Zymed, USA), chicken anti-vimentin (1:2000, Chemicon, France), and rat anti-MECA-32 (1:200, gift from Pr Britta Engelhardt, Switzerland). Additional details appear in the Supplemental Experimental Procedures and Fig. S4.

For pSTAT3 immunolabeling and analysis, mice were injected i.p. with vehicle (5 mM sodium citrate buffer, n = 4 per group), leptin (PeproTech, France) or LAN (Protein Laboratories Rehovot Ltd, Israel) and perfused 45 min later with a 2% paraformaldehyde in 0.1 M phosphate buffer (pH 7.4). Brains were processed for pSTAT3 immunolabeling and

quantification as described previously (Bouret et al., 2012). Additional details appear in the Supplemental Experimental Procedures.

Microdialysis of the hypothalamus

Placement of hypothalamic cannulae and the assessment of ARH and VMH glucose levels in male rats (n = 9) was performed as described previously (Dunn-Meynell et al., 2009) and detailed in the Supplemental Experimental Procedures.

Immunoblotting

Frozen microdissected ME and MBH of mice fed *ad libitum* (n = 3) and those fasting for 24h (n = 3) were immunoblotted as described in the Supplemental Experimental Procedures. Rabbit anti-claudin-1 (1:1000, Zymed, USA), mouse anti-VEGF (1:500, SantaCruz), rat anti-MECA-32 (1:500, Santa Cruz) and goat anti-actin antibodies (1:500, Santa Cruz, France) were used in these experiments.

Statistical analysis

All values are expressed as means $\pm$ SEM. Data were analyzed for statistical significance with SigmaPlot software (Version 11.0), using one-way or two-way ANOVA followed by a Tukey post hoc test when appropriate. P-values of less than 0.05 were considered to be statistically significant.

Supplemental information

The supplemental information includes four figures, Supplemental Experimental Procedures, and Supplemental References.

References

Ambach, G., and Palkovits, M. (1979). The blood supply of the hypothalamus of the rat. In Handbook of the hypothalamus, P.J. Morgane, and J. Panksepp, eds. (New York, Marcel Dekker), pp. 267-377.

Argaw, A.T., Gurfein, B.T., Zhang, Y., Zameer, A., and John, G.R. (2009). VEGF-mediated disruption of endothelial CLN-5 promotes blood-brain barrier breakdown. Proc Natl Acad Sci U S A *106*, 1977-1982.

Banks, W.A. (2006). Blood-brain barrier and energy balance. Obesity (Silver Spring) *14 Suppl 5*, 234S-237S.

Bouret, S.G., Bates, S.H., Chen, S., Myers, M.G., Jr., and Simerly, R.B. (2012). Distinct roles for specific leptin receptor signals in the development of hypothalamic feeding circuits. J Neurosci *32*, 1244-1252.

Carmeliet, P., Dor, Y., Herbert, J.M., Fukumura, D., Brusselmans, K., Dewerchin, M., Neeman, M., Bono, F., Abramovitch, R., Maxwell, P.*, et al.* (1998). Role of HIF-1alpha in hypoxia-mediated apoptosis, cell proliferation and tumour angiogenesis. Nature *394*, 485-490.

Ciofi, P., Garret, M., Lapirot, O., Lafon, P., Loyens, A., Prevot, V., and Levine, J.E. (2009). Brain-endocrine interactions: a microvascular route in the mediobasal hypothalamus. Endocrinology *150*, 5509-5519.

Cowley, M.A., Smart, J.L., Rubinstein, M., Cerdan, M.G., Diano, S., Horvath, T.L., Cone, R.D., and Low, M.J. (2001). Leptin activates anorexigenic POMC neurons through a neural network in the arcuate nucleus. Nature *411*, 480-484.

Cowley, M.A., Smith, R.G., Diano, S., Tschop, M., Pronchuk, N., Grove, K.L., Strasburger, C.J., Bidlingmaier, M., Esterman, M., Heiman, M.L.*, et al.* (2003). The distribution and mechanism of action of ghrelin in the CNS demonstrates a novel hypothalamic circuit regulating energy homeostasis. Neuron *37*, 649-661.

Dunn-Meynell, A.A., Routh, V.H., Kang, L., Gaspers, L., and Levin, B.E. (2002). Glucokinase is the likely mediator of glucosensing in both glucose-excited and glucose-inhibited central neurons. Diabetes *51*, 2056-2065.

Dunn-Meynell, A.A., Sanders, N.M., Compton, D., Becker, T.C., Eiki, J., Zhang, B.B., and Levin, B.E. (2009). Relationship among brain and blood glucose levels and spontaneous and glucoprivic feeding. J Neurosci *29*, 7015-7022.

Elias, C.F., Aschkenasi, C., Lee, C., Kelly, J., Ahima, R.S., Bjorbaek, C., Flier, J.S., Saper, C.B., and Elmquist, J.K. (1999). Leptin differentially regulates NPY and POMC neurons projecting to the lateral hypothalamic area. Neuron *23*, 775-786.

Elmquist, J.K., Coppari, R., Balthasar, N., Ichinose, M., and Lowell, B.B. (2005). Identifying hypothalamic pathways controlling food intake, body weight, and glucose homeostasis. J Comp Neurol *493*, 63-71.

Esser, S., Wolburg, K., Wolburg, H., Breier, G., Kurzchalia, T., and Risau, W. (1998). Vascular endothelial growth factor induces endothelial fenestrations in vitro. J Cell Biol *140*, 947-959.

Flier, J.S. (2004). Obesity wars: molecular progress confronts an expanding epidemic. Cell *116*, 337-350.

Frayling, C., Britton, R., and Dale, N. (2011). ATP-mediated glucosensing by hypothalamic tanycytes. J Physiol *589*, 2275-2286.

Fruehauf, J., Lutzky, J., McDermott, D., Brown, C.K., Meric, J.B., Rosbrook, B., Shalinsky, D.R., Liau, K.F., Niethammer, A.G., Kim, S.*, et al.* (2011). Multicenter, phase II study of axitinib, a selective second-generation inhibitor of vascular endothelial growth factor receptors 1, 2, and 3, in patients with metastatic melanoma. Clin Cancer Res *17*, 7462-7469.

Gao, Q., and Horvath, T.L. (2007). Neurobiology of feeding and energy expenditure. Annu Rev Neurosci *30*, 367-398.

Gerber, H.P., Hillan, K.J., Ryan, A.M., Kowalski, J., Keller, G.A., Rangell, L., Wright, B.D., Radtke, F., Aguet, M., and Ferrara, N. (1999). VEGF is required for growth and survival in neonatal mice. Development *126*, 1149-1159.

Hawkins, B.T., and Davis, T.P. (2005). The blood-brain barrier/neurovascular unit in health and disease. Pharmacol Rev *57*, 173-185.

Hawkins, B.T., Sykes, D.B., and Miller, D.S. (2010). Rapid, reversible modulation of blood-brain barrier P-glycoprotein transport activity by vascular endothelial growth factor. J Neurosci *30*, 1417-1425.

Hill, J.W., Elias, C.F., Fukuda, M., Williams, K.W., Berglund, E.D., Holland, W.L., Cho, Y.R., Chuang, J.C., Xu, Y., Choi, M.*, et al.* (2010). Direct insulin and leptin action on pro-opiomelanocortin neurons is required for normal glucose homeostasis and fertility. Cell Metab *11*, 286-297.

Hokfelt, T., Foster, G., Schultzberg, M., Meister, B., Schalling, M., Goldstein, M., Hemmings, H.C., Jr., Ouimet, C., and Greengard, P. (1988). DARPP-32 as a marker for D-1 dopaminoceptive cells in the rat brain: prenatal development and presence in glial elements (tanycytes) in the basal hypothalamus. AdvExpMedBiol *235*, 65-82.

Ioannidou, S., Deinhardt, K., Miotla, J., Bradley, J., Cheung, E., Samuelsson, S., Ng, Y.S., and Shima, D.T. (2006). An in vitro assay reveals a role for the diaphragm protein PV-1 in endothelial fenestra morphogenesis. Proc Natl Acad Sci U S A *103*, 16770-16775.

Kamba, T., Tam, B.Y., Hashizume, H., Haskell, A., Sennino, B., Mancuso, M.R., Norberg, S.M., O'Brien, S.M., Davis, R.B., Gowen, L.C.*, et al.* (2006). VEGF-dependent plasticity of fenestrated capillaries in the normal adult microvasculature. Am J Physiol Heart Circ Physiol *290*, H560-576.

Lee, D.A., Bedont, J.L., Pak, T., Wang, H., Song, J., Miranda-Angulo, A., Takiar, V., Charubhumi, V., Balordi, F., Takebayashi, H.*, et al.* (2012). Tanycytes of the hypothalamic median eminence form a diet-responsive neurogenic niche. Nat Neurosci *15*, 700-702.

Levin, B.E., Magnan, C., Dunn-Meynell, A., and Le Foll, C. (2011). Metabolic sensing and the brain: who, what, where, and how? Endocrinology *152*, 2552-2557.

Liu, T., Kong, D., Shah, B.P., Ye, C., Koda, S., Saunders, A., Ding, J.B., Yang, Z., Sabatini, B.L., and Lowell, B.B. (2012). Fasting Activation of AgRP Neurons Requires NMDA Receptors and Involves Spinogenesis and Increased Excitatory Tone. Neuron *73*, 511-522.

Maharaj, A.S., Walshe, T.E., Saint-Geniez, M., Venkatesha, S., Maldonado, A.E., Himes, N.C., Matharu, K.S., Karumanchi, S.A., and D'Amore, P.A. (2008). VEGF and TGF-beta are required for the maintenance of the choroid plexus and ependyma. J Exp Med *205*, 491-501.

Mancuso, M.R., Davis, R., Norberg, S.M., O'Brien, S., Sennino, B., Nakahara, T., Yao, V.J., Inai, T., Brooks, P., Freimark, B.*, et al.* (2006). Rapid vascular regrowth in tumors after reversal of VEGF inhibition. J Clin Invest *116*, 2610-2621.

Mullier, A., Bouret, S.G., Prevot, V., and Dehouck, B. (2010). Differential distribution of tight junction proteins suggests a role for tanycytes in blood-hypothalamus barrier regulation in the adult mouse brain. J Comp Neurol *518*, 943-962.

Murakami, T., Felinski, E.A., and Antonetti, D.A. (2009). Occludin phosphorylation and ubiquitination regulate tight junction trafficking and vascular endothelial growth factor-induced permeability. J Biol Chem *284*, 21036-21046.

Neuwelt, E.A., Bauer, B., Fahlke, C., Fricker, G., Iadecola, C., Janigro, D., Leybaert, L., Molnar, Z., O'Donnell, M.E., Povlishock, J.T.*, et al.* (2011). Engaging neuroscience to advance translational research in brain barrier biology. Nat Rev Neurosci *12*, 169-182.

Niv-Spector, L., Gonen-Berger, D., Gourdou, I., Biener, E., Gussakovsky, E.E., Benomar, Y., Ramanujan, K.V., Taouis, M., Herman, B., Callebaut, I.*, et al.* (2005). Identification of the hydrophobic strand in the A-B loop of leptin as major binding site III: implications for large-scale preparation of potent recombinant human and ovine leptin antagonists. Biochem J *391*, 221-230.

Oh, I.S., Shimizu, H., Sato, T., Uehara, Y., Okada, S., and Mori, M. (2005). Molecular mechanisms associated with leptin resistance: n-3 polyunsaturated fatty acids induce alterations in the tight junction of the brain. Cell Metab *1*, 331-341.

Peitz, M., Pfannkuche, K., Rajewsky, K., and Edenhofer, F. (2002). Ability of the hydrophobic FGF and basic TAT peptides to promote cellular uptake of recombinant Cre recombinase: a tool for efficient genetic engineering of mammalian genomes. Proc Natl Acad Sci U S A *99*, 4489-4494.

Pytowski, B., Goldman, J., Persaud, K., Wu, Y., Witte, L., Hicklin, D.J., Skobe, M., Boardman, K.C., and Swartz, M.A. (2005). Complete and specific inhibition of adult lymphatic regeneration by a novel VEGFR-3 neutralizing antibody. J Natl Cancer Inst *97*, 14-21.

Rini, B.I., Wilding, G., Hudes, G., Stadler, W.M., Kim, S., Tarazi, J., Rosbrook, B., Trask, P.C., Wood, L., and Dutcher, J.P. (2009). Phase II study of axitinib in sorafenib-refractory metastatic renal cell carcinoma. J Clin Oncol *27*, 4462-4468.

Rodriguez, E.M., Blazquez, J.L., Pastor, F.E., Pelaez, B., Pena, P., Peruzzo, B., and Amat, P. (2005). Hypothalamic tanycytes: a key component of brain-endocrine interaction. IntRevCytol *247*, 89-164.

Saitou, M., Furuse, M., Sasaki, H., Schulzke, J.D., Fromm, M., Takano, H., Noda, T., and Tsukita, S. (2000). Complex phenotype of mice lacking occludin, a component of tight junction strands. Mol Biol Cell *11*, 4131-4142.

Sawchenko, P.E. (1998). Toward a new neurobiology of energy balance, appetite, and obesity: the anatomists weigh in. J Comp Neurol *402*, 435-441.

Thorens, B., and Larsen, P.J. (2004). Gut-derived signaling molecules and vagal afferents in the control of glucose and energy homeostasis. Curr Opin Clin Nutr Metab Care *7*, 471-478.

Wang, E.S., Teruya-Feldstein, J., Wu, Y., Zhu, Z., Hicklin, D.J., and Moore, M.A. (2004). Targeting autocrine and paracrine VEGF receptor pathways inhibits human lymphoma xenografts in vivo. Blood *104*, 2893-2902.

Zhang, H., Zhang, G., Gonzalez, F.J., Park, S.M., and Cai, D. (2011). Hypoxia-inducible factor directs POMC gene to mediate hypothalamic glucose sensing and energy balance regulation. PLoS Biol *9*, e1001112.
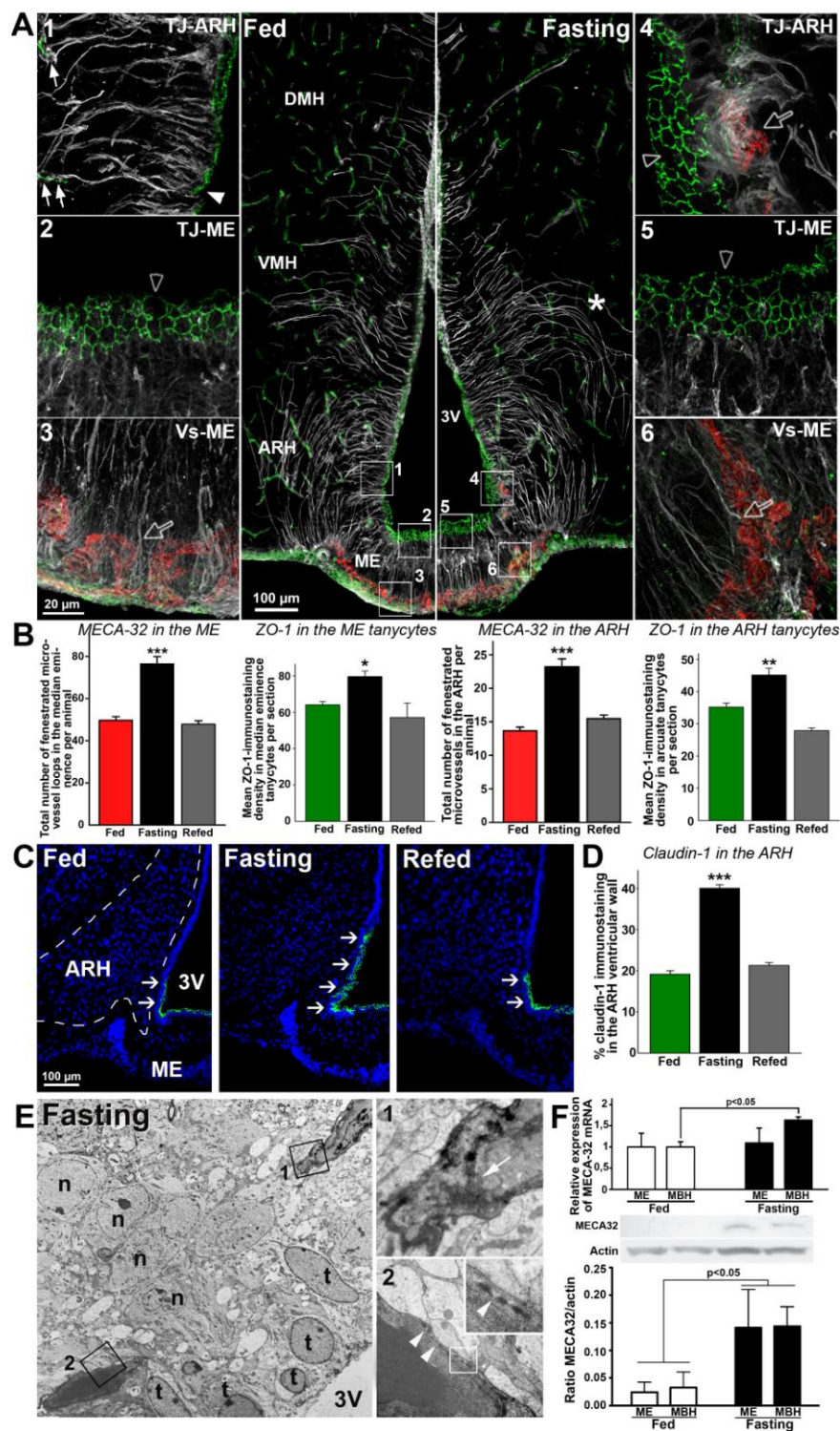
Figures

Figure 1. Fasting-induced fenestration of ME microvessel loops reaching the ARH, and tight junction complex reorganization in ARH tanycytes. (A) Vimentin (white), zonula occludens-1 (ZO-1, green) and MECA-32 (red) immunoreactivity in coronal sections of the hypothalamic tuberal region in fed and fasting mice. Tanycytic tight junction complexes exhibit a diffuse

pattern (arrowheads, inset 1) when interacting with ZO-1-positive blood vessels (arrows, inset 1) and a honeycomb pattern (empty arrowheads, insets 2,4 and 5) when interacting with MECA-32-positive vessels (empty arrows, insets 3,4 and 6). (B) MECA-32-positive microvessel loop number and ZO-1-positive tight junction complex density in the ME and ARH according to nutritional status (n = 4 per group). (C) Distribution of claudin-1 (arrows, green) in coronal sections of the hypothalamic tuberal region in fed, fasting and refed mice. (D) Proportion of the ventricular wall facing the ARH immunolabeled for claudin-1 (n = 4 per group). (E) Electron micrographs from fasting mice showing ARH capillaries with non-fenestrated (arrow, inset 1) and fenestrated endothelia (arrowheads, inset 2); n: neuronal cell bodies; t: tanycyte cell bodies. Scale bar: 10 μm (1μm in insets). (F) Real-time PCR and immunoblotting for MECA-32 and actin from microdissected ME and MBH explants containing the ARH from fed and fasting mice (n = 3-4 per group). *** $p<0.001$; ** $p<0.01$; * $p<0.05$; fasting vs. fed and refed groups. DMH: dorsomedial nucleus of the hypothalamus.
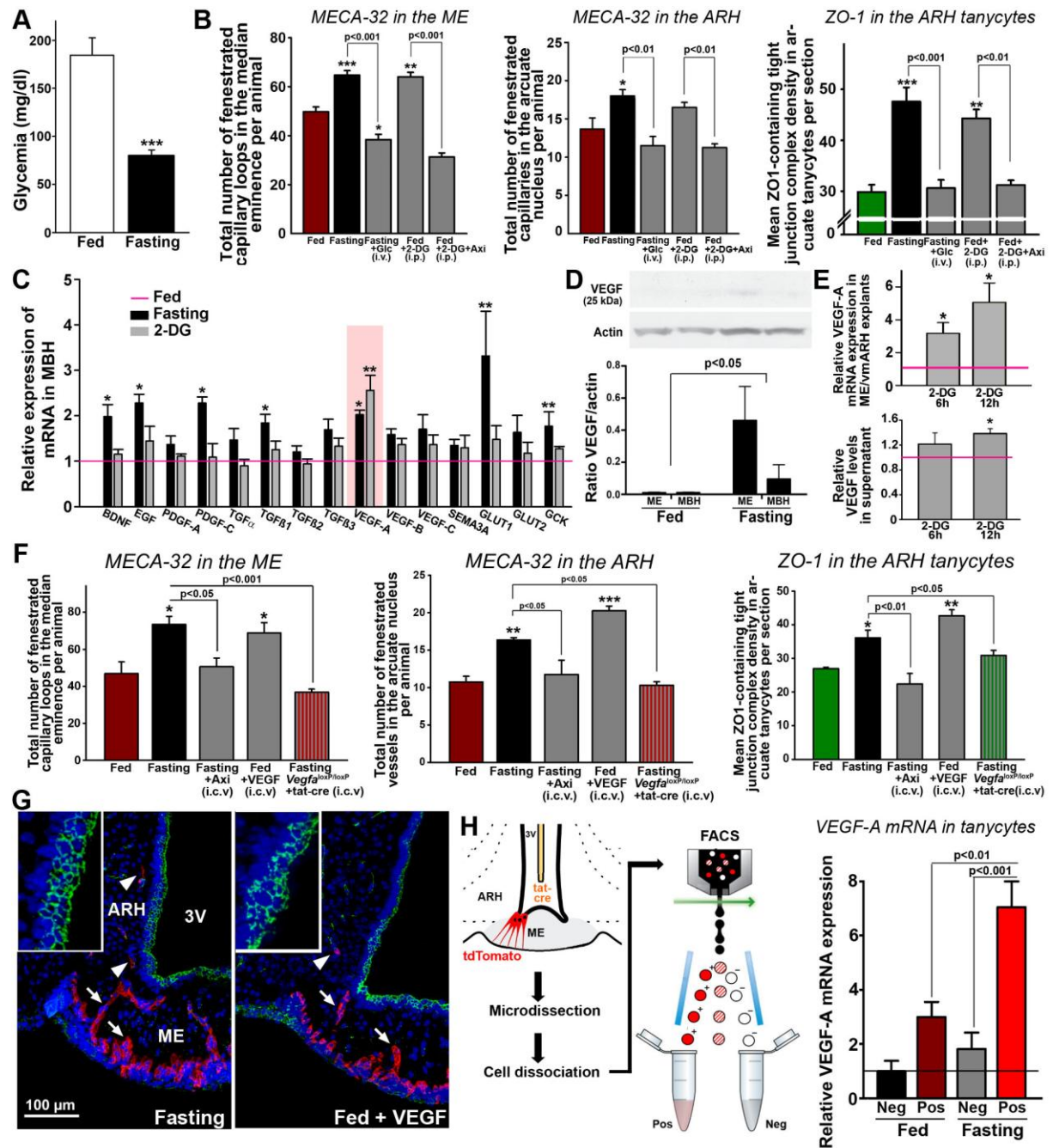
Figure 2. Fasting-induced BHB plasticity is mediated by glucose deprivation and tanycytic VEGF-A expression. (A) Blood glucose levels in fed and fasting mice (n = 6 per group). (B) Structural changes at the blood-CSF barrier in fasting mice infused with glucose (Glc; n = 6) or not (n = 6) and fed mice treated i.p. with 2-DG in the presence (n = 4) or absence of Axitinib (Axi; n = 4) compared to vehicle-treated fed mice (n = 3). (C) Real-time PCR analysis of genes involved in brain plasticity and glucosensing in the MBH of fasting and 2-DG-treated mice, normalized to values in mice fed *ad libitum* (red line) (n = 4 per group). (D) VEGF

accumulates in the ME and MBH of fasting mice, as seen by immunoblotting (n = 3 per group). (E) 2-DG application to ME/vmARH explants increases VEGF secretion when compared to vehicle (red line) (n = 4 per group). (F) Quantification of MECA-32 and ZO-1 immunolabeling in fasting wild-type or $Vegfa^{loxP/loxP}$ mice infused i.c.v. with Axitinib (n = 4) or tat-cre recombinant protein (n = 4), and fed mice treated with VEGF (n = 4) or vehicle (n = 10). (G) MECA-32 (red) and ZO-1 (green) immunolabeling in fasting mice and fed mice treated with VEGF or vehicle. Long MECA-32-positive microvessel loops reach the ependymal layer of the ME (arrows); arrowheads: MECA-32-positive intrainfundibular loop reaching the ARH. (H) Tanycyte isolation by FACS and real-time PCR analysis of VEGF-A mRNA in Tomato-positive (pos; tanycytes) and -negative cells (neg) in fed and fasting mice (n = 4 each). *** p<0.001; ** p<0.01; * p<0.05; various treatment groups vs. untreated fed mice.
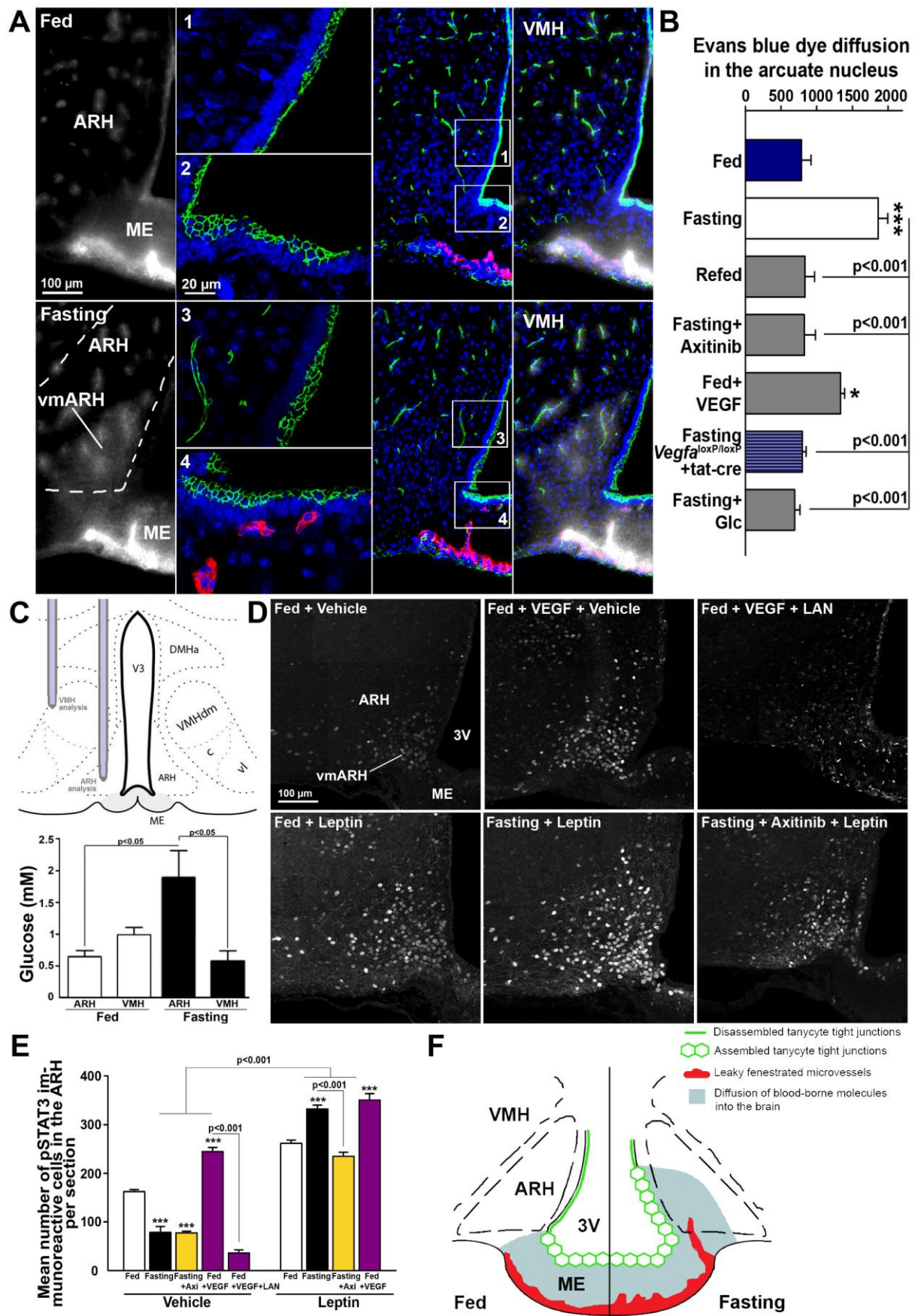
Figure 3. Fasting-induced structural changes at the BHB facilitate the access of blood-borne metabolic signals to the ARH. (A) Evans Blue dye diffusion (gray) and MECA-32 (red) and ZO-1 (green) immunolabeling in the hypothalamic tuberal region in fed and fasting mice. (B) Quantification of Evans Blue diffusion into the ARH in fasting mice infused with Axitinib (n = 4) or glucose (Glc; n = 5), food-deprived tat-cre-treated *Vegfa*$^{loxP/loxP}$ mice (n = 4), fed VEGF-treated mice (n = 5), food-deprived mice after refeeding for 24h (Refed; n = 4) and vehicle-treated fed mice (n = 7). (C) Placement of microdialysis cannulae (upper panel) for the simultaneous measurement of ARH and VMH glucose levels in fed and fasting rats, reported in the bar graph (lower panel, n = 4-5 per group). (D) Distribution of pSTAT3 immunoreactivity (white) in coronal sections of the ARH in fed and fasting mice treated or not with VEGF and Axitinib (Axi) after the i.p. administration of leptin (n = 4 per group), LAN (n = 3) or vehicle (n = 3-4 per group). (E) Quantification of pSTAT3 immunoreactive cells. (F) Structural differences between the ME and ARH of mice fed *ad libitum* and fasting mice, and their effects on the diffusion of blood-borne signals into the brain. *** p<0.001; ** p<0.01; * p<0.05; various treatment groups vs. untreated fed mice.
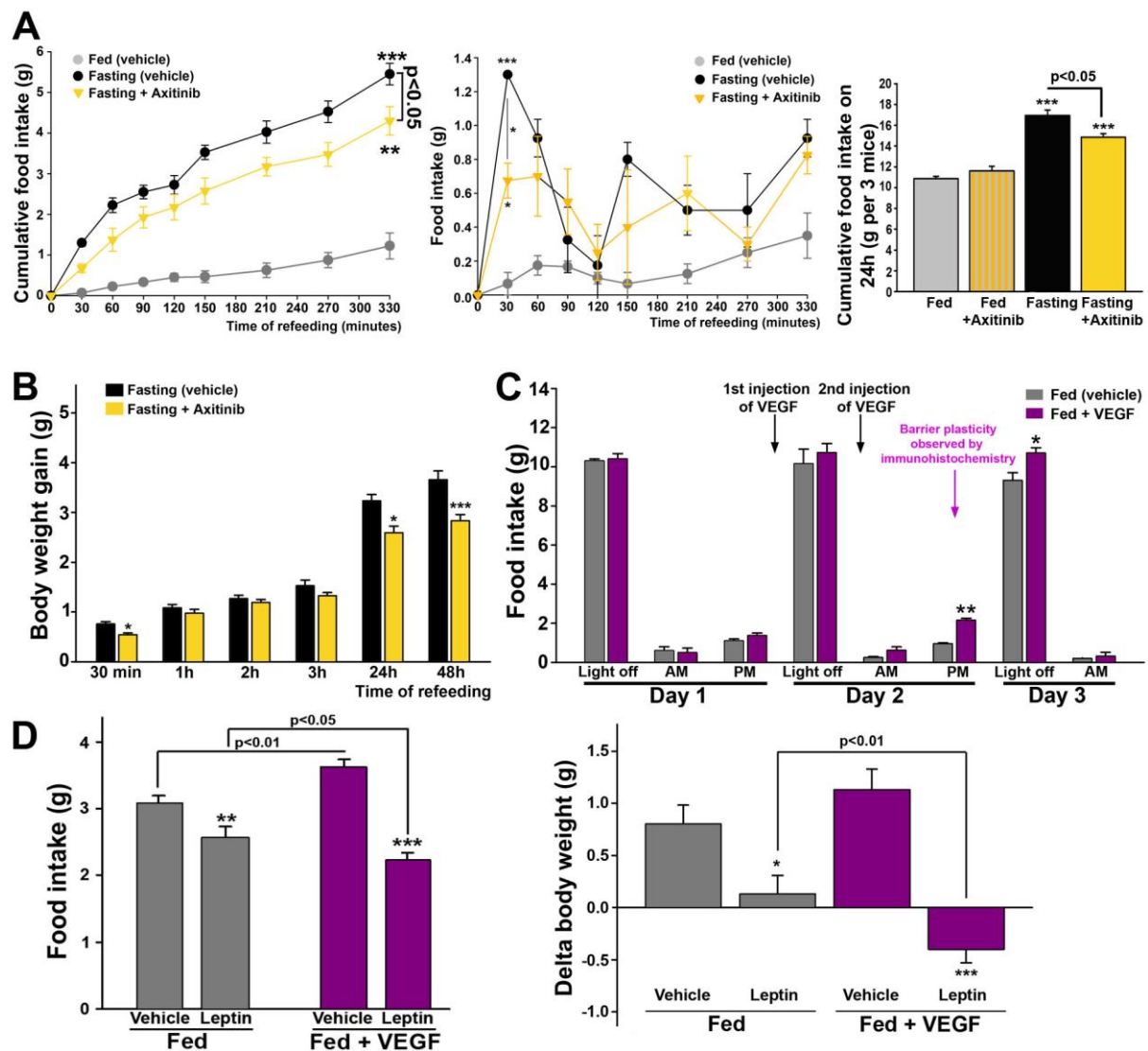
Figure 4. BHB plasticity modulates feeding behavior. (A) Cumulative and absolute food intake in fasting mice with or without i.p. Axitinib injection (orange; n = 4 per group) during refeeding after a 24h fast, and in vehicle-treated (gray; n = 4) or Axitinib-treated mice (gray and yellow stripes; n = 3-4) fed *ad libitum*. (B) Body weight gain during the first 48h of refeeding in mice previously food-deprived for 24h, and that were (orange; n =4) or not treated with Axitinib (black; n = 4). (C) Absolute food intake in mice fed *ad libitum* infused with VEGF (purple; n = 3) or not (gray; n = 4) for 3 days. (D) Anorectic and weight-loss-inducing effects of leptin and vehicle in mice fed *ad libitum* subjected to VEGF treatment or not (n = 10 per group). *** p<0.001; ** p<0.01; * p<0.05; various treatment groups vs. untreated fed mice.